The Nematode Resistance Allele at the *rhg1* Locus Alters the Proteome and Primary Metabolism of Soybean Roots[1][C][W][OA]

Ahmed J. Afzal[2], Aparna Natarajan, Navinder Saini[3], M. Javed Iqbal, Matt Geisler, Hany A. El Shemy[4], Rajsree Mungur, Lothar Willmitzer, and David A. Lightfoot*

Department of Molecular Biology, Microbiology, and Biochemistry (A.J.A., A.N., H.A.E.S., R.M., D.A.L.), Genomics Core Facility and Center for Excellence in Soybean Research, Teaching, and Outreach, Department of Plant Soil and Agricultural Systems (A.J.A., N.S., H.A.E.S., D.A.L.), and Department of Plant Biology (M.G., D.A.L.), Southern Illinois University, Carbondale, Illinois 62901; Institute for Advanced Learning and Research, Institute for Sustainable and Renewable Resources, Danville, Virginia 24540 (M.J.I.); and Max Planck Institute for Molecular Plant Physiology, Potsdam 14476, Germany (R.M., L.W.)

Heterodera glycines, the soybean cyst nematode (SCN), causes the most damaging chronic disease of soybean (*Glycine max*). Host resistance requires the resistance allele at *rhg1*. Resistance destroys the giant cells created in the plant's roots by the nematodes about 24 to 48 h after commencement of feeding. In addition, 4 to 8 d later, a systemic acquired resistance develops that discourages later infestations. The molecular mechanisms that control the *rhg1*-mediated resistance response appear to be multigenic and complex, as judged by transcript abundance changes, even in near isogenic lines (NILs). This study aimed to focus on key posttranscriptional changes by identifying proteins and metabolites that were increased in abundance in both resistant and susceptible NILs. Comparisons were made among NILs 10 d after SCN infestation and without SCN infestation. Two-dimensional gel electrophoresis resolved more than 1,000 protein spots on each gel. Only 30 protein spots with a significant ($P < 0.05$) difference in abundance of 1.5-fold or more were found among the four treatments. The proteins in these spots were picked, trypsin digested, and analyzed using quadrupole time-of-flight tandem mass spectrometry. Protein identifications could be made for 24 of the 30 spots. Four spots contained two proteins, so that 28 distinct proteins were identified. The proteins were grouped into six functional categories. Metabolite analysis by gas chromatography-mass spectrometry identified 131 metabolites, among which 58 were altered by one or more treatment; 28 were involved in primary metabolism. Taken together, the data showed that 17 pathways were altered by the *rhg1* alleles. Pathways altered were associated with systemic acquired resistance-like responses, including xenobiotic, phytoalexin, ascorbate, and inositol metabolism, as well as primary metabolisms like amino acid synthesis and glycolysis. The pathways impacted by the *rhg1* allelic state and SCN infestation agreed with transcript abundance analyses but identified a smaller set of key proteins. Six of the proteins lay within the same small region of the interactome identifying a key set of 159 interacting proteins involved in transcriptional control, nuclear localization, and protein degradation. Finally, two proteins (glucose-6-phosphate isomerase [EC 5.3.1.9] and isoflavone reductase [EC 1.3.1.45]) and two metabolites (maltose and an unknown) differed in resistant and susceptible NILs without SCN infestation and may form the basis of a new assay for the selection of resistance to SCN in soybean.

[1] This work was supported by the U.S. National Science Foundation (grant nos. 04–05819 and USB 6221), the Government of India (fellowship for N.S.), and the Government of Egypt (Egypt-U.S. junior scientist visit grants to H.A.E.S.).

[2] Present address: Department of Horticulture and Crop Science, 2021 Coffey Road, Ohio State University, Columbus, OH 43210.

[3] Present address: Biotechnology Centre, Jawaharlal Nehru Krishi Vishwavidyalaya, Jabalpur-482004, India.

[4] Present address: Faculty of Agriculture Research Park and Department of Biochemistry, Faculty of Agriculture, Cairo University, 12613 Giza, Egypt.

* Corresponding author; e-mail ga4082@siu.edu.

The author responsible for distribution of materials integral to the findings presented in this article in accordance with the policy described in the Instructions for Authors (www.plantphysiol.org) is: David A. Lightfoot (ga4082@siu.edu).

[C] Some figures in this article are displayed in color online but in black and white in the print edition.

[W] The online version of this article contains Web-only data.

[OA] Open Access articles can be viewed online without a subscription.

www.plantphysiol.org/cgi/doi/10.1104/pp.109.138149

Soybean (*Glycine max*) is the world's most important legume crop; it is grown for both oil and protein coproducts (Messina and Liu, 1997). Many natural by-products are also derived from soybean, and several possess significant antimicrobial and pharmacological properties (Dixon and Sumner, 2003). The abundance and variety of soybean's bioactive factors suggest that the species has evolved and been domesticated in the presence of many persistent pathogen populations.

After water deficit, the leading causes of seed yield losses in soybean are biotic stresses from pathogen infections (Wrather et al., 1996). Among soybean pathogens, the soybean cyst nematode (SCN) causes the most damage. Yield losses in the world due to SCN infection have approached $2 billion a year (Niblack et al., 2004) and amounted to $1.5 billion in the United States alone for the 1996 to 1997 period (Chen et al., 2001). SCN preventative measures include crop rota-

tion, the use of resistant cultivars, and nematicides. The use of resistant cultivars provides the most efficient and practical control of SCN.

Soybean breeding has heavily used three plant introductions (PIs) resistant to the cyst nematode (Brucker et al., 2005). The PIs 'PI88788', 'Peking', and 'PI437654' have been shown to carry resistance loci effective against multiple nematode races (Concibido et al., 2004). However, the resistance to SCN was quantitative and controlled by multiple loci. Previously identified were two quantitative trait loci that provided substantial resistance against the SCN Hg type 0 (a biotype of race 3) in near isogenic lines (NILs) derived from Peking via 'Forrest' (Meksem et al., 2001; Ruben et al., 2006). The resistance locus *Rhg4* on linkage group A2 provided resistance against Hg type 0, whereas *rhg1*, the resistance locus on linkage group G, provided some resistance against nematodes of all known races. The *rhg1* locus allele from Peking causes rapid necrosis of the giant cells and the formation of thickened cell walls around the defunct feeding site (syncytium) by 24 to 48 h after the SCN female starts to feed, some 4 to 5 d after infestation of the roots (Alkharouf et al., 2004, 2006; Ithal et al., 2007a, 2007b). The activity of the resistance allele is associated with global changes in transcript abundance (TA) within the syncytium and systemic changes in the root system, with hundreds of transcripts altered. However, in plants, the correlations between transcript, protein, and metabolite abundances are low. Hence, key proteins may have been overlooked by transcript analysis. Furthermore, some proteins can alter the metabolome without alterations in their abundances (Edwards, 1996; Ito et al., 2003; Schad et al., 2005; Mungur, 2008). Therefore, key metabolites may remain undetected. Finally, protein-protein and protein-metabolite interactions are important in many plant responses to the environment (Geisler-Lee et al., 2008). Therefore, key interactions may remain undetected by the transcript analyses reported to date.

The *rhg1* locus appears to be a multifunctional and multigenic locus (Ruben et al., 2006; Afzal, 2007; Iqbal et al., 2009). The locus contained several genes capable of altering the transcriptome, proteome, metabolome, and interactome, including a receptor-like kinase (RLK; Afzal and Lightfoot, 2007) inferred to alter root development (Afzal et al., 2008a, 2008b); an unusual laccase (Iqbal et al., 2009) involved in phenolic metabolism; and a predicted Na/H antiporter. Flanking the locus were two proteins of unknown function, one of which is transcribed in roots (Triwitayakorn et al., 2005; Ruben et al., 2006). Each of the genes was encoded by distinct alleles in resistant soybean compared with susceptible soybean, with significant amino acid and nucleotide changes (Ruben et al., 2006; Afzal et al., 2008a). Analysis in NILs suggested that the resistance alleles of the core set of three linked genes cannot be separated by recombination without the loss of resistance (Afzal, 2007; Afzal et al., 2008a).

Recent progress in the plant disease resistance field has shed light on some resistance (R) proteins and their effector molecules (Martin et al., 2003; for review, see Afzal et al., 2008b). However, the full set of interacting partners implicated in resistance has not been completely decoded. Equally, a number of systematic studies have made progress identifying the transcription abundances that change as a consequence of SCN infection (Alkharouf et al., 2004, 2006; Ithal et al., 2007a; Klink et al., 2007a, 2007b). However, by 2009, there was no report that had addressed the difference in protein abundance in SCN-infested compared with noninfested roots.

Proteomics databases and reference maps for *Medicago truncatula* (Lei et al., 2005) and soybean (Xu et al., 2006) have been constructed using two-dimensional (2D) gel electrophoresis. The 2D gels have also been employed in the identification of proteins expressed during seed filling (Mooney and Thelen, 2004; Hajduch et al., 2005), symbiotic nitrogen fixation (El Yahyaoui et al., 2004), for the detection of glycoproteins using iodine-labeled lectins (Basha and Roberts, 1981), and to explore the consequences of biotic stresses (Lei et al., 2005). However, reports of proteomic analysis of the pathogen-plant relationship have been sparse. These include infection of root hairs with *Bradyrhizobium japonicum* (Wan et al., 2005) and the analysis of pathogenesis-related proteins from tobacco necrosis virus-infected soybean plants (Roggero and Pennazio, 2008).

Recent proteomics projects were encouraged by marked improvements in 2D gel reproducibility. This was achieved mainly by the development of immobilized pH gradient strips (Gorg et al., 2000) and enhanced techniques to obtain soluble proteins (Molloy et al., 1998). Furthermore, image-analysis software with automated statistical analysis eased the laborious process of spot quantification. In addition, in-gel protease digestion, refinement of electrospray ionization tandem mass spectrometry (MS/MS), matrix-assisted laser desorption ionization time-of-flight mass spectrometry (TOF-MS), and protein identification using various databases (National Center for Biotechnology Information [NCBI], Protplot, or organism-specific EST databases) have improved. Accurate identification of femtomolar quantities of proteins is now routine.

The hypotheses explored in this paper were as follows: that expression of the set of candidate genes at *rhg1* might alter the abundance of other plant proteins encoded by unlinked genes; that the altered proteins might form enriched clusters within the interactome; and that protein abundance changes have effects at the metabolite layer. In order to test these hypotheses, the key proteins underlying SCN resistance were identified by 2D gel electrophoresis of total proteins extracted from the roots of NILs with different alleles at *rhg1* infested for 10 d with the SCN Hg type 0. Differences in protein abundance in response to both genotype and pathogen infestation

were noted. TAs were determined for the genes corresponding to the differentially abundant protein spots. An interactome map generated on the basis of orthology between soybean and Arabidopsis (*Arabidopsis thaliana*) proteins helped identify a significant cluster of interacting proteins.

RESULTS

NILs polymorphic across the region encompassing the *rhg1* locus were used for this study. The region between markers BARC-Satt214 (and Satt163) and Satt570 spans 12.7 centimorgans (3.16 Mb), with the *rhg1* candidate gene cluster at about 4 centimorgans, close to the center (Meksem et al., 2001; Ruben et al., 2006; Afzal et al., 2008a). The NIL 34-3 was susceptible to the SCN Hg type used; in contrast, NIL 34-23 was resistant to SCN. NIL genotypes were confirmed by the Southern Illinois University, Carbondale TMD1 marker (GI:218937751) located in the intron of the RLK within the *rhg1* locus (data not shown; Afzal et al., 2008a). Infection of the roots with Hg type 0 nematode at 10 d after infestation (dai) was confirmed by PCR amplification of the nematode 18S ribosomal gene from root-extracted DNA (Fig. 1).

Differentially abundant proteins and metabolites were identified from four two-way comparisons. The first was made between Hg type 0 infested and noninfested SCN resistant NIL 34-23. The second compared the infested resistant NIL 34-23 and the infested susceptible NIL 34-3. The third was made between the infested and noninfested susceptible NIL 34-3. The fourth compared the noninfested resistant NIL 34-23 and noninfested susceptible NIL 34-3. These comparisons were made in an effort to find overexpressed proteins in the susceptible plants infested with SCN Hg type 0 and proteins more abundant in the resistant NIL 34-23. Answers to three fundamental questions were sought. (1) Which proteins and metabolites are differentially abundant in the resistant NIL plant roots as a consequence of SCN infestation? (2) Which proteins and metabolites were at higher abundance in the infested resistant NIL plant roots and not in the infested susceptible NIL plant roots? And (3) were any proteins or metabolites at different abundance in resistant and susceptible NIL plant roots without SCN infestation?

Figure 1. A 2% (w/v) agarose gel after electrophoresis showing the presence (lanes 1 and 2) and absence (lanes 3 and 4) of SCN DNA at 10 d after infestation (lanes 1 and 2) or in noninfested plants (lanes 3 and 4). The SCN 18S ribosomal gene was successfully amplified in infested NILs 34-23 and 34-3 (lanes 1 and 2; top band). No amplification was obtained from DNA extracted from noninfested NILs (lanes 3 and 4). Lane 5 contained the negative control with no template. The bottom band in each lane represents the primers.

Proteome Abundance Analysis

More than 1,000 protein spots were reproducibly resolved on each gel (Fig. 2). The pI for the majority of the spots ranged from pH 4 to 8, whereas the molecular masses for most proteins were between 20 and 100 kD (Fig. 2). Spot comparisons for the two-way analyses were subjected to the Student's *t* test with a significance (*P*) value set at 0.05. A total of 29 spots with a 1.5-fold or higher abundance were chosen for further analysis. Nine spots were overrepresented in the resistant NIL 34-23-infested roots compared with noninfested roots (Table I). Intensities for 12 spots varied between the infested resistant and susceptible NIL roots (34-23-I versus 34-3-I comparison gels; Table II). Four protein spot abundances differed in the susceptible infested roots compared with noninfested roots (34-3-I versus 34-3-NI gels; Table III). Only two spots had higher abundance in the resistant noninfested compared with the susceptible noninfested roots (Table IV), showing that both NIL proteomes were closely isogenic in the absence of pathogen infestation.

For 25 of the 28 spots analyzed, the theoretical and experimental pI and molecular mass deviations were within 20% of the expected values (Tables I–IV). For two of the deviating spots (Glc-6-P isomerase [EC 5.3.1.9] and glutathione *S*-transferase [GST; EC 2.5.1.18]), the extent was marginally greater than 20%, whereas for one spot (ascorbate oxidase [EC 1.10.3.3]), the deviation was significant (Table II) because the predicted protein was a preprotein. The observed differences may be attributed to incorrect N- or C-terminal inferences, novel posttranslational modifications, or length variations between the homologous proteins.

For correctly annotated proteins, there is usually no more than 20% difference between experimental and theoretical molecular mass and pI values (Wan et al., 2005). However, setting 20% as an arbitrary cutoff may lead to the exclusion of some correctly assigned proteins that may migrate to unexpected positions on a 2D gel due to posttranslational modifications (Wan et al., 2005). Furthermore, some spots yielded more than one protein, not an unusual occurrence for 2D analysis of total protein samples involving proteins with similar pI and molecular mass values.

Functional Classification of Proteins

The soybean genome was not yet completely sequenced and annotated in 2009; about 1,200 sequence

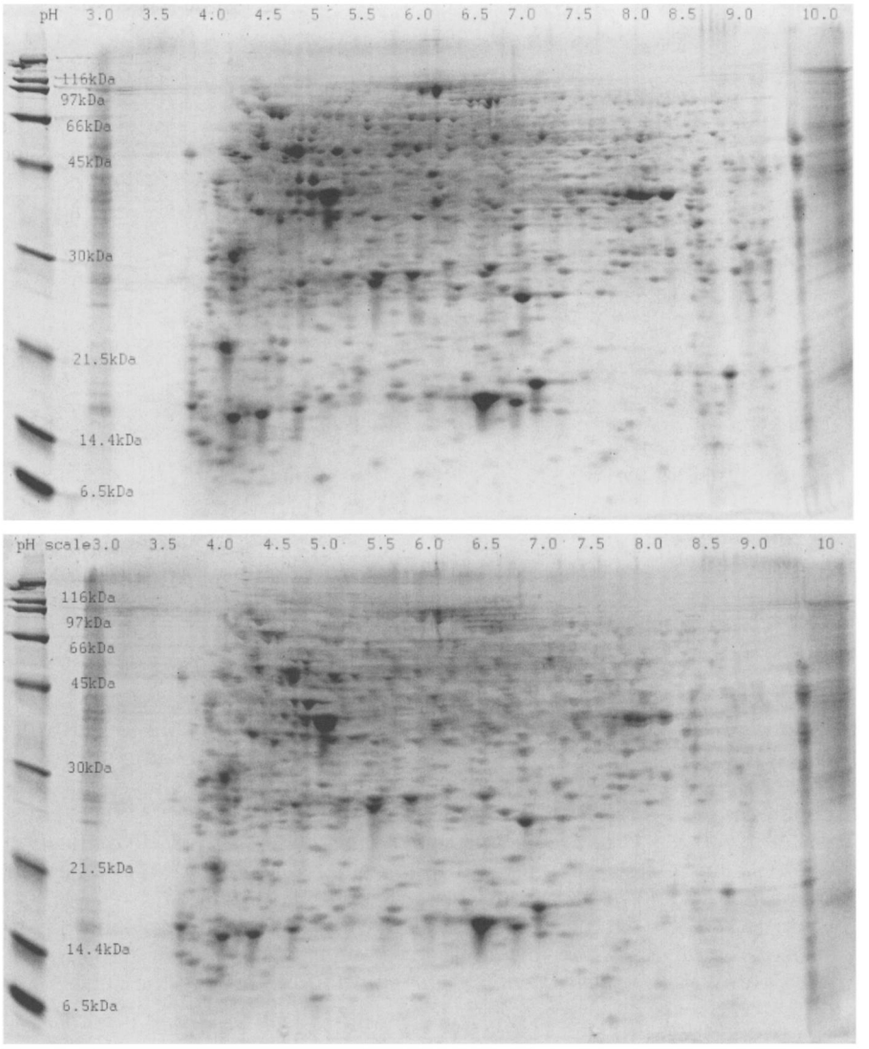

Figure 2. 2D electropherograms obtained from the infested resistant NIL 34-23 (top) and the noninfested resistant NIL 34-23 (bottom). Most protein spots were present under both conditions. The pI for a majority of the spots was in the pH 4 to 8 range, whereas the molecular mass for most proteins was between 20 and 100 kD.

gaps remained. Nevertheless, most of the protein spots of different abundance were successfully identified using the Department of Energy (DOE) sequence, the soybean EST, NCBI, and Swissprot databases. A few sequences had no match to an EST, nucleotide, or protein sequence from soybean. These were identified on the basis of homology to proteins from the Arabidopsis or the *M. truncatula* databases. After identification, the proteins were classified into functional categories (Bevan et al., 1998). The largest functional group was represented by proteins implicated in disease or defense responses (45%), followed by proteins involved in energy-related metabolic functions (29%). About 11% of the proteins belonged to the protein destination and storage category (Fig. 3).

DISCUSSION

Among the significant sample of the high to moderate abundance proteins in soybean roots that could be visualized on 2D gels, finding just 30 significant differences (3%) was surprising. In comparison with metabolites, where 58 of 131 were altered (44%), the number was very low. TA analyses in soybean genotypes that differ by both *rhg1* and *Rhg4* alleles also showed a larger proportion of differences (Alkharouf et al., 2004, 2006; Ithal et al., 2007a; Klink et al., 2007b). Therefore, protein analysis may be focusing on key differences by eliminating TA changes that do not result in protein abundance changes. In addition, the metabolite analyses may show important posttranslational events adding to metabolite changes.

Proteins and Metabolites Altered in Abundance in Roots after SCN Infestation in the Resistant NIL

Among the nine proteins found to be increased by more than 1.5-fold in the roots of infested compared with the noninfested SCN-resistant NIL 34-23 (Table I) were two GSTs. The GST 8 and GST 11 spots had

Table I. *Differentially abundant proteins from the SCN-resistant NIL 34-23-I to NIL 34-23-NI (RI/RNI) comparisons*

R, Resistant; I, infested with SCN; NI, noninfested.

Protein	Accession No.	Mowse Score/ $P < 0.05$	Peptides Matched	Experimental pI, Molecular Mass/Theoretical pI, Molecular Weight	Fold Difference
				measured pI, kD/predicted pI, D	
GST8	Gi11385431	468/24	18	5.5, 27/5.66, 25,851.76[a]	2.18 ± 0.31[b]
Trypsin inhibitor (similar to α-fucosidase)	Gi4313988	107/51	3	5, 18/5.07, 16,658.03[a]	1.58 ± 0.04[b]
Soybean EST induced by salicylic acid	Gi31468505	41/52	2	8.3, 20/10.33, 7,845.53[c]	2.53 ± 0.39[b]
Quinone oxidoreductase	Gi6746930 Gi38191172	81/51	4	7.3, 25/6.84, 21,555.82[a]	2.15 ± 0.34[d]
F1-ATPase	Gi6846042	98/51	4	9.4, 25/9.64, 25,568.81[a]	6.55 ± 2.76[d]
Disease resistance-responsive protein (dirigent-like)	Gi 38191108	99/51	4	9.4, 25/9.88, 20,897.40[a]	6.55 ± 2.76[d]
β-1,3-Endoglucanase	Gi169923	98/51	4	8.3, 37/8.71, 38,111.88[a]	1.72 ± 0.05[b]
Triose-P isomerase	Gi77540216	358/24	10	5.88, 28/5.87, 27,204.11[a]	5.01 ± 0.16[b]
Vegetative storage protein	Gi134146	548/23	23	5.88, 28/6.72, 29,280.41[a]	5.01 ± 0.16[b]
GST11	Gi11385437	120/24	6	6.1, 45/5.89, 25,560.57[c]	2.64 ± 0.30[b]
Putative quinone oxidoreductase	Gi16343485	125/52	3	6.0, 28/6.52, 21,721.82[a]	1.77 ± 0.09[b]

[a]A less than 20% difference between the experimental and theoretical molecular mass and pI values. [b]Significant fold difference. [c]A greater than 20% difference between the experimental and theoretical molecular mass values. [d]Not significant fold difference.

significant differences in molecular mass and pI (Table I). Metabolites in the glutathione pathway included the precursors Gly and Ala that were decreased in abundance (Table V); however, glutathione was not detected. EST analysis of the soybean root library at 8 dai by SCN also suggested a role for GST in resistance to SCN infection (Alkharouf et al., 2004). Similarly, comparative microarray analysis of SCN-infected soybean roots showed increased GST transcripts by 8 dai (Ithal et al., 2007a; Klink et al., 2007). The GST pathway leads to the detoxification of certain compounds during periods of plant stress through conjugation with glutathione. Soybean GSTs mainly conjugate the predominant thiol, homoglutathione (Marrs, 1996). Thus, soybean GSTs may be involved in detoxification reactions during nematode-induced pathogenesis (Alkharouf et al., 2004). Puthoff and coworkers (2003) used an Arabidopsis Affymetrix Genechip to show that following sugar beet cyst nematode (BCN; *Heterodera schactii*) infestation, three of the genes with

Table II. *Differentially abundant proteins from the NIL 34-23-I to NIL 34-3-I (RI/SI) comparisons*

R, Resistant; S, susceptible; I, infested with SCN.

Protein	Accession No.	Mowse Score/ $P < 0.05$	No. of Peptides Matched	Experimental pI, Molecular Mass/Theoretical pI, Molecular Weight	Fold Difference
				measured pI, kD/predicted pI, D	
S-Adenosyl homocysteine hydrolase	Gi37995099	175/51	4	5.1, 50/5.54, 53,374.24[a]	3.33 ± 0.50[b]
Aldehyde dehydrogenase	Gi15337211	291/51	9	5.5, 50/5.77, 56,378.13[a]	3.52 ± 0.86[c]
Enolase	Gi42521309	68/24	4	5.5, 50/5.31, 47,719.28[a]	3.52 ± 0.86[c]
Triose-P isomerase	Gi77540216	354/24	11	5.88, 28/5.87, 27,204.11[a]	2.87 ± 0.31[b]
Glutathione dehydrogenase (ascorbate)	Gi15813814	243/51	9	5.69, 26/5.79, 23,406.93[a]	2.30 ± 0.26[b]
Multicatalytic endopeptidase	Gi24205242	229/51	6	5.1, 25/5.7, 24,031.17[a]	2.65 ± 0.39[b]
Putative p23 cochaperone	Gi4290330	77/51	3	3.3, 24/4.37, 24,957.95[a]	1.99 ± 0.08[b]
mDHAR	Gi51860738	54/52	1	5.69, 40/5.79, 47,380.84[a]	2.75 ± 0.15[b]
Hypothetical disease-responsive protein	Gi6846666	190/51	5	6.4, 25/6.83, 20,593.83[a]	3.35 ± 0.66[c]
Chaperonin	Gi15664434	69/52	4	8.3, 15/7.99, 10,604.39[a]	3.71 ± 0.96[c]
Ascorbate oxidase precursor	Gi22218270	26/24	4	6.15, 25/8.00, 48,098.73[d]	3.26 ± 0.58[b]

[a]A less than 20% difference between the experimental and theoretical molecular mass and pI values. [b]Significant fold difference. [c]Not significant fold difference. [d]A less than 20% difference between the experimental and theoretical molecular mass and pI values.

Table III. *Differentially abundant proteins from the NIL 34-3-I to NIL 34-3-NI (SI/SNI) comparisons*

S, Susceptible; I, infested with SCN; NI, not infested.

Protein	Accession No.	Mowse Score/ $P < 0.05$	No. of Peptides Matched	Experimental pI, Molecular Mass/Theoretical pI, Molecular Weight	Fold Difference
				measured pI, kD/predicted pI, D	
Gly-rich RNA-binding protein	Gi23727906	76/51	3	3.5, 25/4.87, 29,984.81[a]	6.36 ± 0.93[b]
Seed coat peroxidase precursor	Gi2342666	184/25	5	4.4, 40/4.98, 38,106.06[a]	3.66 ± 0.22[b]
Peroxidase	AAD37376	371/51	10	6.7, 40/7.15, 37,614.78[a]	3.52 ± 0.81[b]
Putative mDHAR	Gi27424324	84/52	4	6.3, 50/7.06, 52,501.85[a]	3.02 ± 0.37[b]

[a]A less than 20% difference between the experimental and theoretical molecular mass and pI values. [b]Significant fold difference.

altered TA encoded GSTs. BCN and SCN are closely related species, so the change in GSTs may be an example of an orthologous plant response to nematodes. However, the TA of GSTs in Arabidopsis responds to various stimuli (Marrs, 1996; Coleman et al., 1997; Chen and Singh, 1999) and so may be part of a general defense response.

The protein encoded by an EST (GI:31468505) was increased in abundance by 2.5-fold. The protein did not show similarity to any protein of known function, so it was not in any pathway at MapMan (Thimm et al., 2004). The source EST library was generated after salicylic acid induction (salicylic acid sprayed daily at 2.0 mM for 4 d) in whole 14-d-old seedlings from the SCN-susceptible 'Kefeng 1' plant (Tian et al., 2004). Kefeng 1 was released for innate resistance to *Soybean mosaic virus*. Salicylic acid is a common second messenger protein used by plants to induce resistance responses that are both local and systemic to many pathogens. Here, the existence of a protein product encoded by that mRNA that was 2.5-fold larger than predicted from the genome and EST sequence and an association with SCN resistance were both novel.

Two spots identified as increased in abundance in SCN-infested roots were identical to the soybean NADH-quinone oxidoreductase (QOR; EC 1.6.99.5) isozymes (quinine oxidoreductases; Table I). The enzymes were probably both involved in ubiquinone biosynthesis in roots. No metabolites in the mevalonic acid and quinine pathways were altered in abundance (Table V). However, a cDNA library isolated from laser microdissected syncytia collected 8 d after SCN infestation showed enhanced abundance of the transcript encoding a QOR in a susceptible soybean cultivar (Klink et al., 2005). Similarly, a transcript encoding a QOR was increased in abundance by 4-fold following infestation of Arabidopsis roots with BCN (Puthoff et al., 2003). Increased abundance of QOR transcripts in tomato (*Solanum lycopersicum*) overexpressing the PTO protein has also been observed (Mysore et al., 2003). QOR was shown to act on quinines, a common class of metabolites implicated in energy production, defense against pathogens, and electron transport (Matvienko et al., 2001). QOR reactions produce semiquinones that bind and subsequently inactivate key cellular components such as lipids, proteins, nucleic acids, and carbohydrates (Testa, 1995). Superoxide anions and hydroxyl radicals are also produced through the reaction of semiquinones with molecular oxygen. The superoxide anions and hydroxyl radicals cause enzyme inactivation, trigger membrane lipid peroxidation, and nick DNA. Thus, QOR plays a critical role in cell toxicity associated with the hypersensitive response, particularly in plants combating microbial pathogens (Hammond-Kosack and Jones, 1996). Plant pathogenic cyst nematode genomes like SCN encode several enzymes used in pathogenesis that are bacterial in origin (Ithal et al., 2007a). Perhaps QOR inhibits these enzymes.

One protein with a more than 3.5-fold increase in intensity showed high percentage similarity to a dirigent protein that mediates stereospecific lignin precursor couplings (Table I) and may be involved in the process of cell wall modification/lignification

Table IV. *Differentially abundant proteins from the NIL 34-23-NI to NIL 34-3-NI (RNI/SNI) comparisons*

R, Resistant; S, susceptible; NI, not infested.

Protein	Accession No.	Mowse Score/ $P < 0.05$	No. of Peptides Matched	Experimental pI, Molecular Mass/Theoretical pI, Molecular Weight	Fold Difference
				measured pI, kD/predicted pI, D	
Glc-6-P isomerase	Gi21256302	142/51	6	5.3, 60/5.49, 67,665[a]	3.23 ± 0.26[b]
Isoflavone reductase	Gi6573171	88/52	2	6.1, 30/5.6, 33,980.58[c]	3.04 ± 0.56[d]

[a]A greater than 20% difference between the experimental and theoretical molecular mass values. [b]Significant fold difference. [c]A less than 20% difference between the experimental and theoretical molecular mass and pI values. [d]Borderline between significant and not significant.

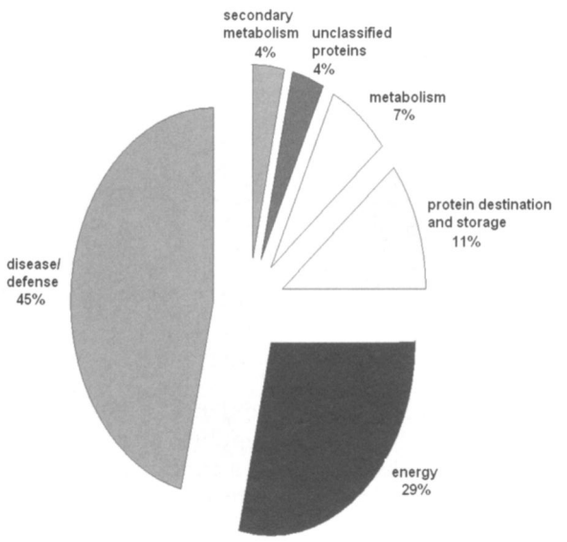

Figure 3. Pie chart showing functional distribution of the proteins identified from 2D-PAGE. About 45% of the identified proteins were involved in disease or defense responses. The classification was based on the functional catalog of plant genes by Bevan et al. (1998).

(Burlat et al., 2001). MapMan (Thimm et al., 2004) placed the enzyme in the lignin and lignan biosynthesis pathway with laccase (EC 1.11.1.7), the enzyme that works in tandem with dirigent proteins. Phe, the amino acid used as a lignin precursor, was decreased in abundance in coordination with the hydroxyl coumaryl alcohol derivative agmatine and the cellulose breakdown product *N*-acetylgalactosamine (Table V). Together, the data suggest that cell walls and protective lignin derivatives are being synthesized to a greater degree in SCN-infested resistant roots. The dirigent proteins have previously been implicated in insect resistance by conifers (Ralph et al., 2006) and cyst nematode resistance in soybean (Klink et al., 2005). Interestingly, the transcript encoding the dirigent-like protein was shown to be decreased in abundance in 3-dai compatible interactions but not in 8-dai compatible interactions (Klink et al., 2007a). A gene encoding a variant laccase is found within the *rhg1* locus (Ruben et al., 2006; Iqbal et al., 2009). Therefore, lignin, lignan, and/or isoflavone biosynthesis may underlie some part of resistance to SCN, perhaps the broad systemic acquired resistance response to secondary infestations from late-hatching eggs (Iqbal et al., 2009).

An additional protein was identified within the dirigent-like protein spot. The protein corresponded to that encoded by a root EST that was predicted to encode the F1-ATPase subunit of mitochondrial ATP synthase (EC 3.6.3.14). Combined, the two proteins appeared to be increased by 6.5-fold. Since ATP synthases are very highly conserved, the spot might also correspond to a protein from the nematode rather than the plant protein, although there were many more plant cells than nematode cells in the samples. ATP synthase mediates ATP production critical to resistance reactions. In addition, a peptide derived from the proteolytic cleavage of the chloroplast ATP synthase can result in the production of the inceptin elicitor that activates plant defense responses in cowpea (*Vigna unguiculata*) during insect herbivory (Schmelz et al., 2006, 2007). Nematode resistance genes can be pleiotropic to genes for resistance to other insect herbivores (Nombela et al., 2003), and there is some evidence for the phenomenon at *Rhg4* in soybean (C.R. Yesudas and D.A. Lightfoot, unpublished data), so this finding may yet be proven significant.

Another protein identified from the comparison of the resistant NIL infested and noninfested was identical to the Kunitz-type trypsin inhibitor, which has strong homology to the α-fucosidase protein (EC 3.2.1.51; Table I; Augur et al., 1995). The *O*-glycosyl hydrolase (EC 3.2.1.-) family encompasses 85 subfamilies. They hydrolyze the glycosidic bond between two or more carbohydrates or between a carbohydrate and a noncarbohydrate moiety. The protein detected here was from family 29, a lysosomal enzyme responsible for hydrolyzing the α-1,6-linked Fuc joined to the reducing end GlcNAc of the carbohydrate moieties of glycoproteins. Among the related metabolites, Glc, sorbose, Man, Gal, Fru, and *N*-acetylgalactosamine decreased in abundance 1.5- to 7.0-fold, while maltose increased 13-fold in resistant NILs with SCN infestations (Table V). Increased TA of the mRNA encoding Kunitz trypsin inhibitor transcript has been observed during plant pathogenesis within the syncytia at 8 dai (Klink et al., 2007a) and in roots at 12 dai (Alkharouf et al., 2006). The protein was associated with the hypersensitive response in leaves of soybeans (Park et al., 2001) and transgeneic tobacco (McManus et al., 1999). The protein was involved in the regulation of nitric oxide synthase and responses to snake venom proteins (see discussion in Park et al., 2001). Therefore, the lysosomal activity of the *O*-glycosyl hydrolase that is a Kunitz trypsin inhibitor seems to be important in root resistance to SCN. Determining the enzyme-specific substrates and molecular bases of the dramatic increase in maltose will be a priority for future work.

Another protein spot increased in abundance corresponded to a β-1,3-endoglucanase (EC 3.2.1.39; Table I). The metabolite substrate Glc was decreased (Table V). The gene family forms a well-characterized group of pathogenesis-related proteins that include cell wall-hydrolyzing enzymes. Endoglucanases have been reported to be activated by both biotic and abiotic stresses. The pathogenesis protein PR2 is a β-1,3-endoglucanase (Graham et al., 2003, 2007). The enzyme acts directly in plant disease resistance through digesting the cell wall of the invading pathogen (Bishop et al., 2005). The released cell wall fragments may also act as elicitors or in resistance, resulting in an accentuated response (Graham et al., 2007).

The most significant changes in protein spot intensity on the 2D gels corresponded to a vegetative

Table V. *Metabolites altered in soybean NILs contrasting at rhg1 (from 131 measured by GC-MS)*

Shown is the fold increase or decrease associated with the NIL genotype (S, susceptible; R, resistant) and the treatment (I, infested with SCN; NI, not infested). Metabolites are grouped by class. Metabolites that could not be named unequivocally were prefixed with y_ and given retention time or class (CHO is the abbreviation for carbohydrate). Metabolites altered more than 5-fold between genotype or by inoculation with SCN are underlined; those increased more than 1.5-fold or decreased more than 1.5-fold are shown in boldface.

Genotypes Compared	SI/SNI	RI/RNI	RI/SI	RNI/SNI
Glc	0.95	0.63	0.67	1.00
Sorbose	0.69	**0.14**	**0.47**	2.32
Man	1.13	0.63	0.76	1.36
Gal	1.20	0.75	0.67	1.08
Fru	0.80	**0.21**	**0.47**	1.80
Maltose	1.63	**13.20**	**0.47**	**0.06**
Trehalose	**0.49**	0.89	1.18	0.65
Glucaric acid	1.22	0.83	**0.46**	0.67
Fumaric acid-like	**0.09**	**0.02**	0.50	2.71
Malonic acid	0.79	0.58	0.91	1.24
Glyceric acid (oxidized glycerol)	0.64	**0.32**	0.73	1.44
Ribonic acid (decarboxylated ribose)	0.76	1.32	1.03	0.59
Citric acid	1.08	0.71	0.46	0.70
Fumaric acid	0.16	0.07	0.62	1.37
N-Acetylgalactosamine	1.41	0.62	0.56	1.27
Phe	0.96	**0.50**	**0.44**	0.84
Asp acid	0.78	0.64	1.03	1.25
Ala	0.65	0.63	0.93	0.96
Val	0.71	0.62	0.89	1.04
Leu	0.64	0.59	0.94	1.00
Ile	0.78	0.62	0.75	0.95
Gly	0.83	**0.36**	0.52	1.22
Glu	0.91	0.69	0.65	0.85
Lys	0.79	0.62	0.80	1.02
3-Hydroxypyruvic acid (deaminated Ser)	0.99	0.53	0.68	1.26
γ-Amino-*N*-butyric acid (decarboxylated Glu)	0.65	0.60	0.68	0.73
Aminovaleric acid (decarboxylated Val)	0.81	1.15	0.80	0.57
Oxoproline	1.06	**0.42**	0.53	1.35
Agmatine (polyamine precursor)	0.85	0.63	0.75	1.01
Inositol	1.03	**0.28**	**0.36**	1.31
Myoinositol	0.93	0.64	**0.36**	0.53
y_fatty acid_414.575	0.64	**0.48**	0.62	0.83
y_213.975	1.88	0.64	**0.50**	1.47
y_217.825	1.11	0.68	0.56	0.90
y_218.325	0.79	0.62	0.73	0.94
y_369.775	0.62	0.92	1.13	0.75
y_438.425	**0.43**	0.53	0.99	0.82
y_451.375	0.81	0.77	0.62	0.65
y_454.325	1.30	0.59	0.50	1.11
y_457.825	0.77	**0.38**	**0.30**	0.62
y_174_460.075	**0.43**	0.80	0.86	**0.46**
y_129_463.175	1.11	1.05	0.59	0.63
y_464.525	0.74	**0.07**	**0.09**	0.94
y_CHO alcohol_469.825	1.09	0.66	0.51	0.85
y_472.575	0.64	**0.30**	**0.33**	0.70
y_478.975	0.55	0.71	**0.34**	**0.26**
y_481.675	**0.49**	0.59	**0.31**	**0.26**
y_531.625	0.92	0.74	**0.50**	0.62
y_CHO_535.325	0.80	**0.23**	**0.24**	0.84
y_540.675	1.34	1.23	0.64	0.69
y_174_547.575	0.58	0.46	0.64	0.81
y_CHO_556.425	1.41	**0.26**	**0.45**	2.40
y_CHO_608.175	0.66	**0.21**	0.52	1.61
y_174_632.975	0.59	0.88	1.38	0.93
y_CHO_645.575	1.94	1.44	0.58	0.78
y_149_677.825	0.94	0.68	0.52	0.71
y_CHO_854.975	**2.85**	**7.54**	0.77	**0.29**
y_204_863.325	1.10	1.56	1.49	1.06

storage protein (VSP) and a triose-P isomerase (EC 5.3.1.1; Fig. 4; Table I; Xu et al., 2006). The enzyme is at a key point in glycolysis and gluconeogenesis. Several metabolites, substrates, and end products in those pathways were decreased in abundance (Table V); only maltose and ribonic acid were increased. The enzyme is a target of glutathionylation by GST in Arabidopsis (Ito et al., 2003) and was increased in abundance by 2-fold in peach (*Prunus persica*) fruit after salicylic acid treatment (Chan et al., 2007). Therefore, this protein may be involved in the energetics of resistance. Considering the VSP, in both soybean and Arabidopsis the VSP was induced as a consequence of methyl jasmonate treatment, wounding, and insect feeding (Liu et al., 2005). The recombinant protein added to the diets of acid gut insects can cause a significant delay in development and an increase in mortality. The transcript accumulated in Arabidopsis plants infested with the SBN (Puthoff et al., 2003). Therefore the VSP may act as a deterrent to feeding.

Proteins and Metabolites Altered by SCN Infestation of Resistant Compared with Susceptible NIL Roots

Twelve spots had differential abundance (Table II). Three of the 12 proteins were increased in abundance in the inoculated resistant NIL roots (previous section). There was a 2.7-fold increase in triose-P isomerase and VSP spot intensity (Fig. 4) and a 3.3-fold increase in a dirigent-like protein (Table II). Therefore, these proteins were increased by SCN infestation in resistant but not susceptible NILs. Proteins increasing abundance in response to both genotype and infestation are likely to be important to resistance to SCN.

Among the proteins altered only in the resistant-to-susceptible infested NIL comparison (increased by the resistance allele at *rhg1* independent of SCN infestation), the enolase (EC 4.2.1.11) protein was increased 3-fold (Table II). The enzyme converts 2-phosphoglycerate into the shikimate pathway precursor, phospho*enol*pyruvate, during both glycolysis and gluconeogenesis. The direct metabolites were not detected by gas chromatography-mass spectrometry (GC-MS), but several sugars and Krebs cycle acids, citric acid and fumaric acid, were reduced in the resistant NIL (Table V). Therefore, increased glycolysis may occur in the SCN resistance response as it does during both tomato defense against the powdery mildew fungus (Li et al., 2006) and symbiosis between soybean root hairs infected with *Bradyrhizobium japonicum* (Wan et al., 2005).

Another protein increased in abundance was the aldehyde dehydrogenase-1A1-like enzyme (EC 1.2.1…) involved in the conjugation of isoprenoids in plants to various products, including carotenoids and terpenoids. The precursor metabolites inositol and myoinositol were significantly decreased in the resistant roots (Table V). Furthermore, plants with mutations in this enzyme accumulated hydrogen peroxide, suggesting a role for this protein in plant defense against oxidative stress (Kirche et al., 2004). Conversely, elevated hydrogen peroxide can mediate the nonenzymatic condensation of lignins and lignans in association with dirigent proteins. Suppression of susceptibility to toxin inhibition of mitochondrial metabolism in T-cytoplasm maize (*Zea mays*) by interference with the production of the Turf-13 protein can be mediated by aldehyde dehydrogenases. Therefore, there are several mechanisms by which this enzyme might contribute to resistance to SCN through constitutively higher abundance in resistant genotypes.

A 3-fold increase in the *S*-adenosyl homocysteine hydrolase (SAH; EC 3.3.1.1) protein spot was detected in SCN-infested resistant NILs (Table II). This enzyme is involved in converting adenosylselenohomocysteine to adenosine and selenohomocysteine, substrates in many methyltransferase reactions. None of the metabolites in this pathway was detected by GC-MS. Methylation reactions are involved in the synthesis and activation of many antimicrobial compounds (Mitsui et al., 1997). SAH can inhibit the synthesis of ethylene, slowing senescence and the hypersensitive response. Transcripts encoding SAHs were increased during the hypersensitive response in cassava (*Manihot esculenta*; Kemp et al., 2005) and alfalfa (*Medicago sativa*; Edwards, 1996). Therefore, the protein seems

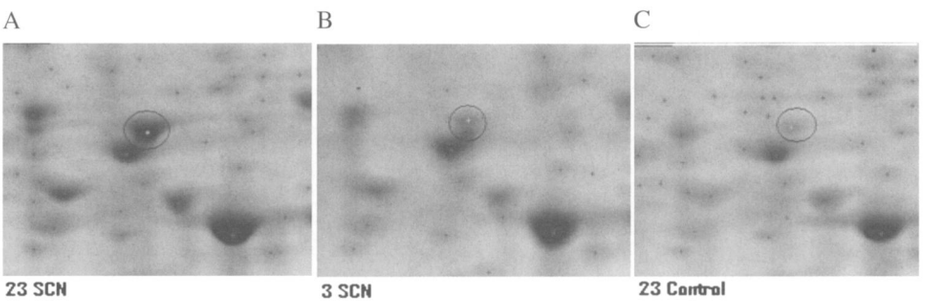

Figure 4. The regions of three 2D electropherograms displaying differences in protein expression between the infested resistant NIL (A), infested susceptible NIL (B), and noninfested resistant NIL (C). The circled spots show quantitative differences in all three gels. Two proteins were identified within the spot. These were the vegetative storage protein and triose-P isomerase.

likely to contribute to resistance by being constitutively increased in resistant NIL roots.

Three of seven enzymes in the ascorbate metabolism pathway were constitutively more abundant in resistant NIL roots. Ascorbate oxidase, dehydroascorbate reductase (DHAR; EC 1.8.5.1; Fig. 5A), and monodehydroascorbate reductase (mDHAR; EC 1.6.5.4) were identified (Table II). The precursor threonate was slightly decreased by about 1.4-fold in the resistant NILs (inferred by Fourier transform ion cyclotron resonance MS; Afzal, 2007). The oxidation of ascorbic acid to the toxic dehydro-L-ascorbic acid has roles in impeding insect growth and development (Felton and Summers, 1993). DHAR and mDHAR are involved in the detoxification of hydrogen peroxide and were increased in barley (*Hordeum vulgare*) genotypes resistant to powdery mildew (El Zahaby et al., 1995) and maize overexpressing a superoxide dismutase gene (EC 1.15.1.1; Kingston-Smith and Foyer, 2000). Tobacco expressing a foreign mDHAR showed increased abiotic stress resistance (El Tayeb et al., 2007). Therefore, constitutively higher expression of the ascorbate pathway in resistant NILs may be involved in innate resistance to SCN.

A multicatalytic endopeptidase protein was increased (Table II). The protein was highly similar (89% identity, 96% similarity) to an EST from embryos of SCN-resistant soybean 'Jack' that encoded the 20S proteasome β-subunit A1 (EC 3.4.25.1), a central hub in the protein-to-protein interactome (Supplemental Table S1). The 20S proteasome was involved in the breakdown of oxidatively modified or damaged proteins (Giulivi et al., 1994; Lee et al., 2006) and in the activation of SAGA-dependent transcription (Shukla et al., 2009). In rice (*Oryza sativa*) challenged with *Rhizoctonia solani*, this protein was increased in both resistant and susceptible genotypes, although the increase in abundance was higher in the resistant line. A constitutive increase in the multicatalytic endopeptidase protein abundance in resistant soybean NILs may be involved in maintaining the resistance response by degrading nematode proteins, by reducing or repairing oxidative damage by activating transcription of a subset of genes, or by changing the rates of deactivation and degradation of proteins according to their contribution to defense.

Two protein spots with increased intensities were members of the chaperonin (EC 3.6.4.9) family of proteins (Table II), a 10-kD-like chaperonin and a 23-kD-like cochaperonin that assist in protein folding and are heat shock proteins (HSPs; Sangster and Queitsch, 2005). Several HSPs were identified as activated upon pathogen infection (Sangster and Queitsch, 2005; Wan et al., 2005; Klink et al., 2007a, 2007b). Overexpression of HSP70 in the resistant plants was reported to reduce root mass in Arabidopsis (Sung and Guy, 2003). In this study and previously, shorter roots and lower root masses were seen in plants that underwent incompatible reactions (Brucker et al., 2005; Afzal et al., 2008a). Furthermore, a different chaperonin appeared to interact with the RLK at *rhg1*. Therefore, the chaperonins present at higher abundance in resistant roots may underlie three phenomena; part of the SCN resistance; the reduced seedling vigor associated with resistance (Brucker et al., 2005; Afzal et al., 2008a); and the lower seed yield that results (Yuan et al., 2002).

Proteins Induced by SCN in the Infested Susceptible NIL Roots

Proteins in this class might be part of a defeated defense response or proteins induced by signals from SCN to root cells. Four proteins were identified (Table

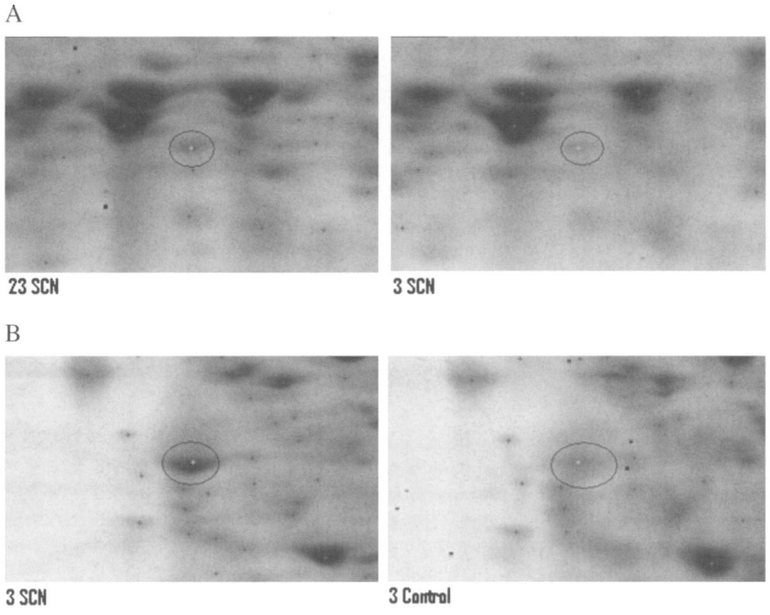

Figure 5. The regions of three 2D electropherograms displaying differences in protein expression between the infested resistant NIL and the infested susceptible NIL. The protein circled in A was glutathione dehydrogenase (Table II). B shows differentially abundant proteins in the susceptible infested compared with the susceptible noninfested NILs. The protein circled was a peroxidase (Table III).

III). One, mDHAR, had been detected as constitutively increased in the resistant genotype. The mDHAR spot, therefore, was increased in both the resistant infested and susceptible infested NILs, but to a lesser degree. Therefore, the protein increase was a general response to SCN infestation enhanced by resistance to SCN directed by *rhg1*.

A spot with a 6-fold increased abundance was identified as a Gly-rich RNA-binding protein (RBP; Table III). RBP TAs were increased by a number of external stimuli, including wounding, abscisic acid, dehydration, stress, mercuric chloride treatment, and infection with TMV (Brady et al., 1993; Naqvi et al., 1998). The role of nucleus-localized RBP in adjustments to changing internal and external stimuli may be based upon interactions with several RNAs, proteins, and kinases. Therefore, the change in protein abundance during a compatible reaction with SCN may be part of a general response to infection or may be directed by the nematode.

Two spots corresponding to peroxidase (EC 1.11.1.7) proteins were increased in abundance (Table III; Fig. 5B). The substrates were inferred to be inorganic chemicals not detected by GC-MS. Peroxidase TAs have dual roles in plant defense, sometimes decreased in abundance to channel resources to more urgent regulatory needs (Moy et al., 2004) or increased, as in 8-d post-SCN infestation syncytial cells compared with root cells (Klink et al., 2007b). Peroxidases may have an active role in wheat (*Triticum aestivum*) stem rust disease (Seevers et al., 1971; Tyagi et al., 2000). The increase in peroxidase isozymes during pathogen infection may restrict pathogen growth. Alternatively, peroxidases could be involved in the synthesis of plant phenolics or the detoxification of peroxide substrates (Seevers et al., 1971).

Protein Comparisons between Noninfested Resistant and Noninfested Susceptible NILs

Proteins in this class were expected to be constitutively increased by the presence of the resistance allele at *rhg1*. Only Glc-6-P isomerase and isoflavone reductase showed increased abundance in the comparison (Table IV). Glc-6-P isomerase was a glycolytic enzyme that converts Glc-6-P into Fru-6-P. The metabolite Fru and product sorbose were increased about 2-fold, while the substrate precursor maltose decreased 13-fold in resistant NILs (Table V). Previously, Glc-6-P isomerase was among a number of glycolytic enzymes with increased abundance in cereals in response to the sheath blight fungus (Danson et al., 2000). Therefore, increased glycolysis in roots might contribute to greater readiness to mount a resistance response to SCN.

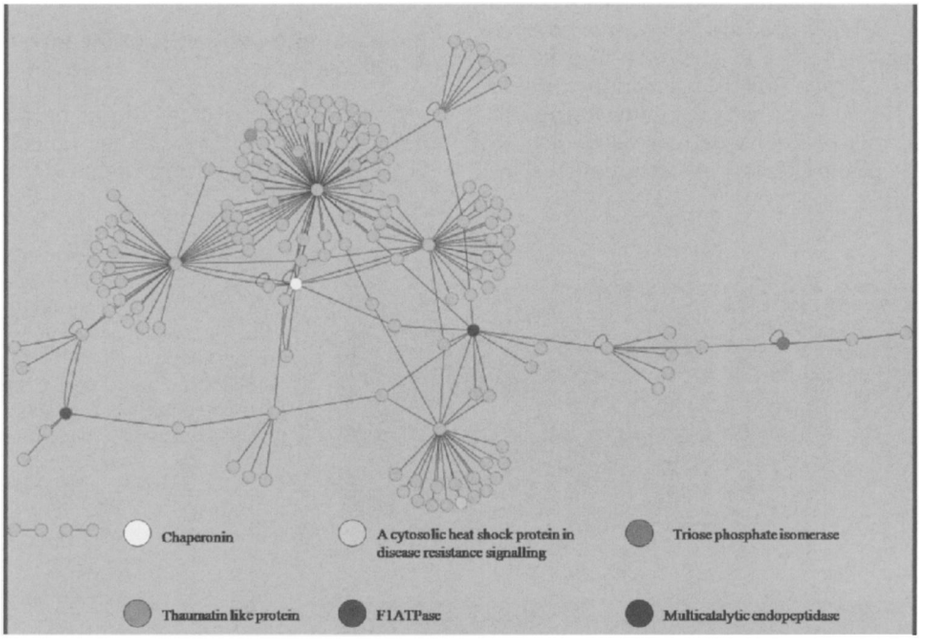

Figure 6. Part of the predicted interactome for soybean showing six proteins from the 2D gel analysis (chaperonin, F1-ATPase, multicatalytic endopeptidase, TL protein, cytosolic HSP, and triose-P isomerase). The interactome was extended by one node to include 159 nodes (proteins) and 194 edges (interactions; Supplemental Table S1). Two proteins with previously characterized roles in disease resistance were identified within this part of the interactome: the TL protein induced in response to fungal pathogens (blue) and a cytosolic HSP in disease resistance signaling (green). All six proteins interacted through two to seven intermediate partners (for pink spot identification, see Supplemental Table S1). Autoregulation was predicted for the triose-P isomerase and the chaperonin. [See online article for color version of this figure.]

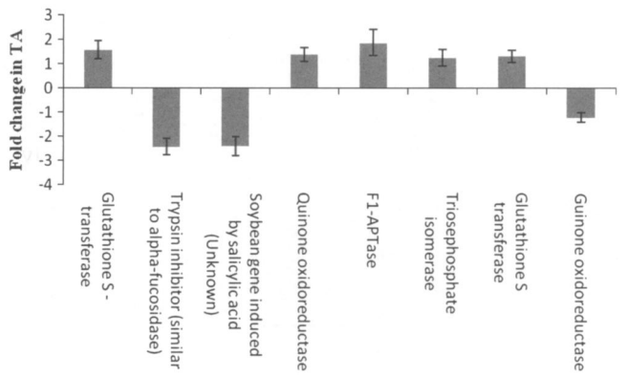

Figure 7. Relative TA ratios measured by quantitative reverse transcription-PCR. The fold change in relative TA in the resistant SCN-infested NIL compared with the resistant noninfested NIL is shown for 10 plant replicates pooled after tissue grinding for RNA extraction. Data shown are means ± SD from three technical replicates.

Isoflavone reductase (EC 1.3.1.45) was also implicated in readiness against SCN infestation by a 3-fold increase (Table IV). The precursor Phe was slightly decreased in abundance in resistant genotypes (Table V), possibly as a result of the more active isoflavone synthesis. Isoflavone reductase accumulation in plants increases with increased resistance toward pathogen infection (Kuc, 1995; Ithal et al., 2007a) by increased production of phytoalexins and deposition of lignin (Keen, 1992). Interactions with the laccases and dirigent proteins are expected. Therefore, the isoflavonoid phytoalexin synthesis pathways are strongly inferred to be under the control of the *rhg1* locus.

Interactome Analysis

Ortholog analysis was conducted on 31,921 proteins from Arabidopsis (from The Arabidopsis Information Resource) and 62,199 proteins from soybean (from the DOE at www.phytozome.net). Shown at SoyGD (http://soybeangenome.siu.edu) was the score that was the likelihood for direct orthology ("in-paralogs"), while the other members of the gene family were "out-paralogs" (multiple orthologs among species without a clear in-paralog). If a single protein could not be assigned as the best ortholog, InParanoid (Remm et al., 2001) assigned it to clusters as one-to-many (one protein in one species having many orthologs in the other) and many-to-many (many proteins in one species having many orthologs in the other). For clarity here, only one-to-one orthologs (in-paralogs) were considered. This more stringent predicted soybean interactome was compared with the proteins altered in abundance by SCN infestation (Fig. 6). Among them, proteins were spread into many clusters, as expected from pathway analysis (19 enzymes in 17 pathways). However, initially, four proteins were clustered in one small part of the interactome, comprising 16 proteins within the interactome map. Since this clustering represented a massive enrichment (40,000-fold over random), their interactions were expanded by another node. After two iterations, two more proteins were added. Thus, from the huge soybean interactome, a small portion of 159 proteins with significant resistance to SCN was identified, with an enrichment of 4,000-fold, suggesting significance for the protein cluster.

The predicted interactome showed that chaperonin, F1-ATPase, multicatalytic endopeptidase, thaumatin-like (TL) protein, cytosolic HSP, and triose-P isomerase were interacting indirectly through two to seven intermediates (Fig. 6). The cluster of all potential interacting neighbors showed 159 proteins in total, with 194 interactions. The protein functions included transcription factors, chaperonins, signal transduction factors, and metabolism involved in energy generation (Supplemental Table S1). The four proteins in the cluster with the most interacting partners were a GTP-binding family protein (28 partners), importin α-2 subunit (64 partners), importin β-2 subunit (22 partners), and 26S proteasome non-ATPase regulatory subunit 3a (21 partners). Therefore, the regulation of protein degradation and transport of proteins across the nuclear membranes may be important aspects of resistance to SCN.

Among the 159 proteins predicted to interact were many proteins previously associated with disease resistance. One was the TL protein induced by SCN as well as in response to pathogens (displayed in blue in Fig. 6). TL proteins were previously shown to be

Table VI. *Fold change in TA from the NIL 34-23-I to NIL 34-23-NI (RI/RNI) comparisons*

SD values are for each comparison performed in triplicate. R, Resistant; I, infested with SCN; NI, not infested.

Gene Code	Gene Name	Fold Change	SD
A1a	Glutathione *S*-transferase	1.57	0.38
A2	Trypsin inhibitor (similar to α-fucosidase)	−2.43	0.34
A3b	Soybean gene induced by salicylic acid (unknown)	−2.41	0.39
A4	Quinone oxidoreductase	1.38	0.28
A5	F1-ATPase	1.87	0.53
A7	Triose-P isomerase	1.26	0.34
A8	Glutathione *S*-transferase	1.31	0.24
A9	Quinone oxidoreductase	−1.2	0.20

Table VII. *Fold change in TA from the NIL 34-23-I to NIL 34-3-I (RI/SI) comparisons*

SD values are for each comparison calculated from assays performed in triplicate. R, Resistant; S, susceptible; I, infested with SCN.

Gene Code	Gene Name	Fold Change	SD
B1	*S*-Adenosyl homocysteine hydrolase	−13.5	0.26
B2	Aldehyde dehydrogenase	16.32	0.77
B4	Glutathione dehydrogenase (ascorbate)	1.33	0.45
B5	Multicatalytic endopeptidase	1.75	0.56
B7	Monodehydroascorbate reductase	1.16	0.41
B8	Hypothetical disease-responsive protein	−1.65	0.40
B10	Chaperonin	−1.11	0.42

defense proteins that reduced the permeability of the cell walls to pathogenic fungi (Trudel et al., 1998). The TL protein in soybean roots was predicted to interact with the nuclear importin α-2 subunit-like node (Fig. 6; Supplemental Table S1), a nodal protein. The chaperonin detected to be changed in protein abundance by SCN was also predicted to interact at this node. Therefore, the regulation of transport and modification of both plant and nematode-secreted proteins across the nuclear membranes during resistance to SCN will be a focus of future studies.

The second protein previously linked to disease resistance was a cytosolic HSP (AT4G11260.1; displayed in green in Fig. 6). This protein interacted with the 26S proteasome non-ATPase regulatory subunit 3a (Table II). In Arabidopsis, HSP90 was required for complete RPS2-mediated signaling in response to pathogens (Takahashi et al., 2003) and was shown to interact with the disease resistance signaling component SGT1b (Azevedo et al., 2002). Therefore, during resistance to SCN, protein-protein interactions were predicted to play an important role in cellular functions. Eventually, the interactome map for soybean may be used to predict which proteins in a network respond to various external stimuli and to design new mechanisms of resistance.

Comparison of TA between Infested and Noninfested Resistant NILS

Seven of the 19 genes that encoded enzymes in pathways were chosen to compare protein with TAs, because mRNA-specific primers that produced single amplicons could be designed. GST8 (gene 1a; 1.57 ± 0.38), quinine oxidoreductase (1.38 ± 0.27), F1-ATPase (1.87 ± 0.53), triose-P isomerase (1.25 ± 0.34), and GST11 (gene 8; 1.31 ± 0.24) were increased in TA when the comparison was between the infested and noninfested NILs. There was agreement between the 2D gel and real-time quantitative PCR results for these genes. However, the gene transcripts encoding trypsin inhibitor (−2.43 ± 0.34), the EST induced by salicylic acid (−2.41 ± 0.39), and quinine oxidoreductase (−1.2 ± 0.20) were decreased in TA but increased in protein abundance (Fig. 7; Table VI). The protein abundance increase in response to SCN was inferred to be a posttranscriptional event for these three proteins that may reflect differences between protein and RNA half-lives (Yu et al., 2007). Correlations between transcript and protein abundances have mostly been weak (Greenbaum et al., 2003; Yu et al., 2007). Therefore, root resistance to SCN was shown to be derived from changes in both TA and protein abundance.

TA Differences between Resistant and Susceptible NILs Infested with SCN

A similar uncoupling between TA and protein abundance was observed when the mRNA abundance in infested resistant NIL 34-23 and infested susceptible NIL 34-3 was compared. Of seven genes encoding proteins increased in abundance, four were increased in TA: aldehyde dehydrogenase (16.32 ± 0.76), glutathione dehydrogenase (ascorbate; 1.33 ± 0.45), multicatalytic endopeptidase (1.75 ± 0.56), and mDHAR (1.16 ± 0.41). However, three genes encoding *S*-adenosyl homocysteine hydrolase (−13.5 ± 0.25), hypothetical disease-responsive protein (−1.65 ± 0.40), and chaperonin (−1.11 ± 0.42) were found decreased in TA (Table VII; Fig. 8). Therefore, both root resistance and susceptibility to SCN were shown to be derived from changes jointly in TA and protein abundance.

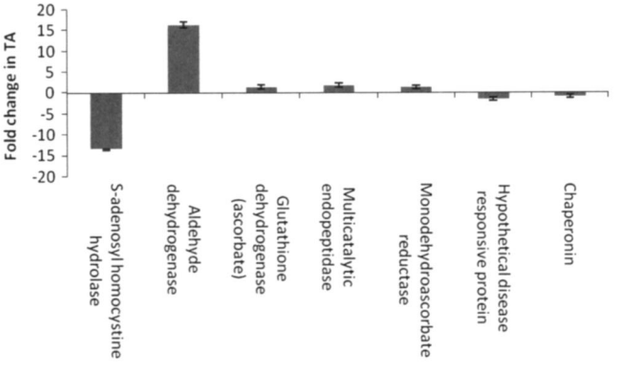

Figure 8. Relative TA ratios measured by quantitative reverse transcription-PCR. The fold change in relative TA in the resistant infested NIL compared with the susceptible infested NIL is shown for 10 plant replicates pooled after tissue grinding for RNA extraction. Data shown are means ± SD from three technical replicates.

CONCLUSION

Numerous attempts to determine the key transcripts involved in SCN resistance in soybean have been made (Alkharouf et al., 2004, 2006; Klink et al., 2005, 2007a, 2007b). Variations in experimental design included analysis of compatible and incompatible interactions, plant responses to resistant and susceptible SCN biotypes, and analysis of transcript variations at different days post inoculation. None of the studies thus far sought to determine changes in actual protein abundance as a function of SCN infection. Previous studies relied heavily on genomic tools, mainly microarray analysis using soybean Affymetrix chips to measure TA. One weakness of TA analysis is that the abundances of transcripts and of the respective proteins may not correlate well. In this study, there was limited correlation between some transcripts and their encoded proteins but more between proteins and their substrates or metabolites. Therefore, results obtained from transcriptomic, proteomic, and metabolomic analyses must be integrated and compared with the interactomes to elucidate the nature of resistance to SCN and other phenomena. This study showed that differentially abundant proteins exist in the context of genotype and reaction following SCN infection and laid the groundwork for a systems biology approach to SCN resistance. In addition, proteins and metabolites in roots were discovered that may be used to predict the resistance of seedlings without SCN infestation at high throughput. Future research will explore the usefulness of these biomarkers further.

MATERIALS AND METHODS

Materials

Seeds of soybean (*Glycine max*) were obtained from Southern Illinois University at Carbondale. Seeds of NIL 34-23 (resistant haplotype between markers Satt214 and Satt570) and NIL 34-3 (susceptible haplotype between Satt214 and Satt570) were used at the F5:13 generation. Genotypes were *rhg1rhg1Rhg4Rhg4* for NIL 34-23 and *Rhg1Rhg1Rhg4Rhg4* for NIL 34-3 (if *rhg1*-derived resistance was recessive; for the counter evidence, see Afzal et al., 2008a).

Growth Conditions

Soybean plants were grown in tubes (5 cm × 30 cm) placed in buckets of sand with 20 tubes in a completely randomized design. Each tube contained a 1:1 ratio of sand to soil mix. The buckets were placed in a water bath to maintain root zone temperature at 24°C and grown in a 14-h-light cycle, with aerial daytime temperature of 30°C and nighttime temperature of 22°C. The humidity was maintained at approximately 40% to 50% (v/v).

Infection with Hg type 0 SCN populations consisted of infestation of the root zone of 14-d-old seedlings with 2,000 eggs in 2 mL of water. Noninfested plants were provided the same volume of water. For this Hg type, female indices (FI) were 'PI54840' (FI 7%), PI88788 (FI 2%), 'PI90763' (FI 1%), PI437654 (FI 0%), 'PI209332' (FI 1%), 'PI89772' (FI 2%), 'PI548316' (FI 8%), and 'PI548402' (FI 3%). Therefore, the standard differentials showed this HG type to be 0 (Niblack et al., 2004), corresponding to a biotype of race 3.

Soybean plants (infested and noninfested) were removed from the cones at 10 dai. The cones were transferred to a cold-water (4°C) container and briefly soaked until the sand-soil mixture became loose. The plant roots were subsequently cleaned with distilled water, blotted dry, cut from the shoots, and stored in a −80°C freezer.

DNA Extraction

DNA was isolated following a modified protocol by Afzal et al. (2008a). Briefly, 100 mg of plant tissue was homogenized and frozen, and 600 μL of preheated (65°C) extraction buffer (Tris-HCl [pH 8.0; 100 mM], EDTA [pH 8.0; 20 mM], NaCl [1.4 M], cetyl-trimethyl-ammonium bromide [2%, w/v], and 2-mercaptoethanol [0.4%, v/v]) was added. The samples were incubated at 65°C for 1 h, cooled, and centrifuged at 10,000*g* for 15 min. The supernatant was decanted, and 5 μL of RNase (5 mg mL^{-1}) was added and incubated at 37°C for 1 h. The DNA in the aqueous phase was purified by phenol:chloroform: isoamyl alcohol (25:24:1) extraction followed by chloroform:isoamyl alcohol (24:1). DNA was precipitated by the addition of isopropanol and centrifugation at 12,000*g* for 5 min. The DNA pellets were washed twice with 70% (v/v) ethanol, dried, and finally dissolved in 30 μL of Tris buffer. DNA concentrations were calculated by measuring A_{260}.

NIL Genotype and Infection Confirmation

About 50 ng of DNA was used for microsatellite analysis according to Yuan et al. (2002). The microsatellite marker TMD1 (GI:218937751; forward primer 5′-TGGTGGTGATGTTGAAGCAG-3′; reverse primer 5′-TAGCAGCAGTT-GACATCAAC-3′) was used to differentiate between the resistant and susceptible NILs. To confirm infection in SCN-infested plants at 10 dai and lack thereof in the noninfested NILs, PCR amplification used the *Heterodera glycines* 18S ribosomal gene primer pair (Forward-HG-18S, 5′-TATTCACCACC-TACCTGCTGTCCT-3′; Reverse-HG-18S, 5′-GCAGCCATACACAGGCTTT-CACAT-3′).

Total Protein Extraction and Quantification

Total protein extraction followed Hurkman and Tanaka (1986) and Hajduch et al. (2005). Briefly, frozen root samples from 10 plants were pooled together, ground to a fine powder, and 2 g of tissue was resuspended in 5 mL of Tris-buffered phenol (pH 8.8) and 5 mL of extraction buffer (0.1 M Tris-HCl, pH 8.8, 0.4% [v/v] β-mercaptoethanol, 10 mM EDTA, and 0.9 M Suc). The solution was vortexed vigorously and centrifuged at 5,000*g* for 15 min. After removal of the top phase (phenol), the bottom phase was back extracted with Tris-buffered phenol (5 mL) and an equal volume of the extraction buffer. Proteins were pelleted by centrifugation at 20,000*g* for 20 min and washed according to Hajduch et al. (2005). The pellet was dried and resuspended in the DeStreak rehydration agent (GE Healthcare). Protein concentration was determined using a noninterfering protein assay (Sheffield et al., 2006).

2D Gel Electrophoresis and Image Analysis

Protein extracts (275 μg) from infested NILs or noninfested NILs (34-23 and 34-3) were used for the 2D electrophoretic analysis. Briefly, samples were initially hydrated overnight on 17-cm Bio-Rad immobilized pH gradient gel strips (pH 3–10), and isoelectric focusing was performed using the Protean IEF Cell (Bio-Rad). Equilibration of the strips was according to the manufacturer's instructions. Linear SDS-PAGE gradient gels (8%–16%, w/v) were used to resolve proteins in the second dimension. A Bio-Rad Protean II apparatus was used for gel electrophoresis at 15 mA cm^{-1} for 30 min, followed by 25 mA cm^{-1} for approximately 5 h at ambient temperature (20°C ± 2°C). Gels were washed with distilled water and stained with SYPRO Ruby. SYPRO Ruby fluorescent dye used for gel staining provided both higher sensitivity and a broad linear range for accurate protein quantification and detection (Sheffield et al., 2006).

Image Analysis and Spot Picking

Acquisition of gel images used a high-resolution laser scanner (Typhoon 9410 from GE Healthcare) and a CCD camera linked to a GelPix protein spot excision system (Genetix). Images were analyzed with the Imagemaster 2D software (GE Healthcare). The analysis was fully automated unless there was a need to manually edit unresolved spots. Identical spots from the compared gels were chosen by assigning landmarks to each gel. The volume for each protein spot was normalized against the total spot intensity. The Student's *t* test ($P < 0.05$) was used to determine whether spot intensities between treatments were significantly different. Differentially abundant spots were excised manually or with the GelPix system.

Protein Digestion and Cleanup

Proteins were digested in-gel as described previously (Gabelica et al., 2002), with the exception that digestion was carried out at 37°C overnight with 6 mg mL^{-1} trypsin (Promega) in 50 mM NH_4HCO_3. The samples were initially extracted with 30 μL of 1% (v/v) formic acid and 2% (v/v) methyl cyanide followed by incubation at 30°C for 30 min on a shaking platform. For the second extraction, 60% (v/v) acetonitrile was used. The pooled extractions were separated into aliquots, lyophilized, and stored. Aliquots were resuspended in 2% (v/v) acetonitrile and 1% (v/v) formic acid solution for use. Proteins were further purified and cleaned using a 10-μL C18 ZipTip (Millipore) according to the manufacturer.

Database Searching

Proteins were identified via peptide sequencing using electrospray ionization MS/MS as described previously (Chen, 2006). Analyst QS software (Applied Biosystems) was used for spectral processing. The peptides were searched against the soybean and *Medicago truncatula* EST databases (downloaded from NCBI in January 2006), the nonredundant NCBI database, and the Swissprot database using MASCOT version 1.9. Input parameters for variable and fixed modifications were specified as oxidation of Met and carbamidomethylation of Cys, respectively. Positive identification was based on the following: (1) number of peptide sequences identified in a protein; (2) calculated and theoretical pI/kD; and (3) total MASCOT and MOWSE scores (http://www.matrixscience.com/help/scoring_help.html) at $P < 0.05$. Protein sequences derived from EST databases or without significant matches were searched against the NCBI BLASTX and TBLASTX databases for evidence of orthology and against the DOE soybean peptide library (www.phytozome.net) for evidence of identity.

Quantitative PCR Analysis

Total RNA was isolated using Trizol (Invitrogen) from both mock-infected and SCN-infected root samples. Total RNA was treated with DNaseI, and the absence of DNA was confirmed by PCR amplification using intron-flanking primers before reverse transcription. Reverse transcriptase SuperScript II (Invitrogen) was used to generate first-strand cDNA following the manufacturer's protocol. Primer pairs for the genes corresponding to differentially expressed proteins were designed using the IDT primer design tool (www.idtdna.com). Primers are listed in Supplemental Table S2. SYBR Green (iQ SYBR Green Supermix; Bio-Rad) was used to measure the number of amplicons after the quantitative PCR. The experiments were performed in triplicate. The soybean tubulin gene was used as an internal control (Iqbal et al., 2009). At the end of each experiment, the melting curve for each amplicon was determined at 62°C to 95°C, with readings every 1°C. The $2^{-\Delta\Delta CT}$ method was used to analyze the relative changes in TA as described previously (Livak and Schmittgen, 2001).

Metabolite Extraction, Identification, and Pathway Analysis

Metabolites were extracted and identified from nine replicated plant samples using adapted standard operating practices for GC-TOF-MS analysis of plant extracts as reviewed by Mungur (2008). Briefly, 15 mg of freeze-dried root tissue was ground in 2 mL of extraction mix (methanol:water, 1:1, v/v) on ice, shaken for 4 to 6 min at 4°C, and centrifuged for 2 min at 14,000*g*. About 1 mL of supernatant was collected as two aliquots, which were dried in a vacuum centrifuge. All samples and replicates were stored at –20°C under argon or nitrogen until further processing. The dried extracts were dissolved in 5 μL of methoxamine hydrochloride (20 mg mL^{-1} pyridine) and incubated at 30°C for 90 min with continuous shaking. Then, 45 μL of *N*-methyl-*N*-trimethylsilyltrifluoroacetamide was added to derivatize polar functional groups at 37°C for 30 min.

GC-TOF-MS (Leco Pegasus II GC-TOF mass spectrometer; Leco) analyses were performed on an HP 5890 gas chromatograph with tapered, deactivated split/splitless liners containing glasswool (Agilent) and 1.5 μL of splitless injection at 230°C injector temperature. Before each injection, the liner was rinsed with a pure *N*-methyl-*N*-trimethylsilyltrifluoroacetamide injection (1 μL). The gas chromatograph was operated at a constant flow of 2 mL min^{-1} helium with a 30-m × 0.32-mm (i.d.) × 0.25-μm MDN35 column (Macherey-Nagel). The temperature gradient started at 80°C, was held isocratic for 2 min, and subsequently was ramped at 15°C min^{-1} to a final temperature of 330°C, which was held for 6 min. Twenty spectra per second were recorded between mass-to-charge ratios 85 and 500. Peak identification and quantification were performed using the Pegasus software package ChromaTOF 1.61 (Leco). Retention time shifts were corrected by linear interpolation using known metabolites as reference markers. All files were subsequently processed against a reference that was generated using a signal-to-noise threshold of 10 with automated peak identification based on mass spectral comparison with a standard NIST 98 library and available in-house customized mass spectral libraries.

GC-MS identified 131 metabolites, among which 58 were significantly altered by one or more treatment. Of the 58, 27 could not be unequivocally identified but 31 were named. A full description of the metabolite analysis will be published elsewhere. Here, metabolite data were examined for concordance with the pathways in which the protein enzymes were altered in abundance. The analysis used MapMan tuned for the soybean proteins that were known enzymes (Goffard and Weiller, 2006) or their Arabidopsis (*Arabidopsis thaliana*) orthologs (Thimm et al., 2004). MapMan showed the enzymes in pathways with their metabolites.

Protein-Protein Interactome Analysis

A Linux-based software, InParanoid (Remm et al., 2001), was used to detect orthologs between Arabidopsis and soybean. InParanoid works on the NCBI-based BLAST server, where 100% orthology is assigned for an E-value of 0.01 or lower. The first round of the program used BLOSSUM45 as the scoring matrix. The second and third rounds used BLOSSUM62 and BLOSSUM80, respectively. Proteins with greatest orthology (percentage similarity) between the two species were used for the analysis. Protein annotations for the orthologs of soybean were imported from http://www.biomart.org, which contained curated information for Arabidopsis proteins from The Arabidopsis Information Resource and Ensemble. Proteins of soybean that showed clear orthology to Arabidopsis were superimposed onto the Arabidopsis interactome kindly provided by Dr. Matt Geisler. Cytoscape 2.5.1 was used to build the interactome.

Supplemental Data

The following materials are available in the online version of this article.

Supplemental Table S1. The predicted interactome viewed in Figure 6.

Supplemental Table S2. Primers used in reverse transcription-PCR.

ACKNOWLEDGMENTS

We thank Dr. P. Gibson, O. Myers Jr., and M. Schmidt for assistance with germplasm development and maintenance from 1991 to 2000 and Gary and Mary Kinsel for assistance with protein analysis and interpretation. The support of the Southern Illinois University, Carbondale, College of Agriculture and Office of the Vice Chancellor for Research to D.A.L., A.J.A., and M.J.I. is appreciated. We thank the DOE Community Joint Sequencing Program for release of the whole genome shotgun reads and scaffolds.

Received March 5, 2009; accepted May 3, 2009; published May 8, 2009.

LITERATURE CITED

Afzal AJ (2007) Structure-function analysis of a candidate receptor like kinase protein in soybean cyst nematode resistance and identification of accessory proteins involved in plant defense. PhD thesis. Southern Illinois University, Carbondale, IL

Afzal AJ, Lightfoot DA (2007) Soybean disease resistance protein RHG1-LRR domain expressed, purified and refolded from *Escherichia coli* inclusion bodies: preparation for a functional analysis. Protein Expr Purif **53:** 346–355

Afzal AJ, Saini N, Srour A, Lightfoot DA (2008a) The multigeneic *rhg1* locus: a model for the effects on root development, nematode resistance and recombination suppression. Nature Precedings http://hdl.handle.net/10101/npre.2008.2726.1 (December 1, 2008)

Afzal AJ, Wood AJ, Lightfoot DA (2008b) Plant receptor-like serine threonine kinases: roles in signaling and plant defense. Mol Plant Microbe Interact **21:** 507–517

Alkharouf N, Khan R, Matthews B (2004) Analysis of expressed sequence tags from roots of resistant soybean infected by the soybean cyst nematode. Genome **47:** 380–388

Alkharouf NW, Klink VP, Chouikha IB, Beard HS, MacDonald MH, Meyer S, Knap HT, Khan R, Matthews BF (2006) Time-course microarray analyses reveal global changes in gene expression of susceptible *Glycine max* (soybean) roots during infection by *Heterodera glycines* (soybean cyst nematode). Planta **224:** 838–852

Augur C, Stiefel V, Darvill A, Albersheim P, Puigdomenech P (1995) Molecular-cloning and pattern of expression of an alpha-l-fucosidase gene from pea seedlings. J Biol Chem **270:** 24839–24843

Azevedo C, Sadanandom A, Kitagawa K, Freialdenhoven A, Shirasu K, Schulze-Lefert P (2002) The RAR1 interactor SGT1, an essential component of R gene-triggered disease resistance. Science **295:** 2073–2076

Basha SM, Roberts RM (1981) The glycoproteins of plant seeds: analysis by two-dimensional polyacrylamide gel electrophoresis and by their lectin-binding properties. Plant Physiol **67:** 936–939

Bevan M, Bancroft I, Bent E, Love K, Goodman H, Dean C, Bergkamp R, Dirkse W, Van Staveren M, Stiekema W, et al (1998) Analysis of 1.9 Mb of contiguous sequence from chromosome 4 of *Arabidopsis thaliana*. Nature **391:** 485–488

Bishop JG, Ripoll DR, Bashir S, Damasceno CM, Seeds JD, Rose JK (2005) Selection on Glycine beta-1,3-endoglucanase genes differentially inhibited by a Phytophthora glucanase inhibitor protein. Genetics **169:** 1009–1019

Brady KP, Darvill AG, Albersheim P (1993) Activation of a tobacco glycine-rich protein gene by a fungal glucan preparation. Plant J **4:** 517–524

Brucker E, Carlson S, Wright E, Niblack T, Diers B (2005) *Rhg1* alleles from soybean PI 437654 and PI 88788 respond differentially to isolates of *Heterodera glycines* in the greenhouse. Theor Appl Genet **111:** 44–49

Burlat V, Kwon M, Davin LB, Lewis NG (2001) Dirigent proteins and dirigent sites in lignifying tissues. Phytochemistry **57:** 883–897

Chan ZL, Qin GZ, Xu XB, Li BQ, Tian SP (2007) Proteome approach to characterize proteins induced by antagonist yeast and salicylic acid in peach fruit. J Proteome Res **6:** 1677–1688

Chen SX (2006) Rapid protein identification using direct infusion nanoelectrospray ionization mass spectrometry. Proteomics **6:** 16–25

Chen SY, Porter PM, Orf JH, Reese CD, Stienstra WC, Young ND, Walgenbach DD, Schaus PJ, Arlt TJ, Breitenbach FR (2001) Soybean cyst nematode population development and associated soybean yields of resistant and susceptible cultivars in Minnesota. Plant Dis **85:** 760–766

Chen W, Singh KB (1999) The auxin, hydrogen peroxide and salicylic acid induced expression of the Arabidopsis GST6 promoter is mediated in part by an *ocs* element. Plant J **19:** 667–677

Coleman JOD, Blake-Kalff MMA, Davies TGE (1997) Detoxification of xenobiotics by plants: chemical modification and vacuolar compartmentation. Trends Plant Sci **2:** 144–151

Concibido VC, Diers BW, Arelli PR (2004) A decade of QTL mapping for cyst nematode resistance in soybean. Crop Sci **44:** 1121–1131

Danson J, Wasano K, Nose A (2000) Infection of rice plants with the sheath blight fungus causes an activation of pentose phosphate and glycolytic pathways. Eur J Plant Pathol **106:** 555–561

Dixon RA, Sumner LW (2003) Legume natural products: understanding and manipulating complex pathways for human and animal health. Plant Physiol **131:** 878–885

Edwards R (1996) S-Adenosyl-L-methionine metabolism in alfalfa cell cultures following treatment with fungal elicitors. Phytochemistry **43:** 1163–1169

El Tayeb AE, Kawano M, Badawi GH, Kaminaka H, Sakata T, Shibahara T, Inanaga S, Tanaka K (2007) Overexpression of monodehydroascorbate reductase in transgenic tobacco confers enhanced tolerance to ozone, salt and polyethylene glycol stresses. Planta **225:** 1255–1264

El Yahyaoui F, Küster H, Ben Amor B, Hohnjec N, Pühler A, Becker A, Gouzy J, Vernié T, Gough C, Niebel A, et al (2004) Expression profiling in *Medicago truncatula* identifies more than 750 genes differentially expressed during nodulation, including many potential regulators of the symbiotic program. Plant Physiol **136:** 3159–3176

El Zahaby HM, Gullner G, Kiraly Z (1995) Effects of powdery mildew infection of barley on the ascorbate-glutathione cycle and other antioxidants in different host-pathogen interactions. Phytopathology **85:** 1225–1230

Felton GW, Summers CB (1993) Potential role of ascorbate oxidase as a plant defense protein against insect herbivory. J Chem Ecol **19:** 1553–1568

Gabelica V, Vreuls C, Filee P, Duval V, Joris B, De Pauw E (2002) Advantages and drawbacks of nanospray for studying noncovalent protein-DNA complexes by mass spectrometry. Rapid Commun Mass Spectrom **16:** 1723–1728

Geisler-Lee J, O'Toole N, Ammar R, Provart NJ, Millar AH, Geisler MA (2008) Predicted interactome for *Arabidopsis thaliana*. Plant Physiol **145:** 317–329

Giulivi C, Pacifici RE, Davies KJA (1994) Exposure of hydrophobic moieties promotes the selective degradation of hydrogen peroxide-modified hemoglobin by the multicatalytic proteinase complex, proteasome. Arch Biochem Biophys **311:** 329–341

Goffard N, Weiller G (2006) Extending MapMan: application to legume genome arrays. Bioinformatics **22:** 2958–2959

Gorg A, Obermaier C, Boguth G, Harder A, Scheibe B, Wildgruber R, Weiss W (2000) The current state of two-dimensional electrophoresis with immobilized pH gradients. Electrophoresis **21:** 1037–1053

Graham MY, Weidner J, Wheeler K, Pelow ML, Graham TL (2003) Induced expression of pathogenesis-related protein genes in soybean by wounding and the *Phytophthora sojae* cell wall glucan elicitor. Physiol Mol Plant Pathol **63:** 141–149

Graham TL, Subramanian S, Graham MY, Yu O (2007) RNAi silencing of genes for elicitation or biosynthesis of 5-deoxyisoflavonoids suppresses race specific resistance and hypersensitive cell death in *Phytophthora sojae* infected tissues. Plant Physiol **144:** 728–740

Greenbaum D, Colangelo C, Williams K, Gerstein M (2003) Comparing protein abundance and mRNA expression levels on a genomic scale. Genome Biol **4:** 117

Hajduch M, Ganapathy A, Stein JW, Thelen JJ (2005) A systematic proteomic study of seed filling in soybean: establishment of high-resolution two-dimensional reference maps, expression profiles, and an interactive proteome database. Plant Physiol **137:** 1397–1419

Hammond-Kosack KE, Jones JDG (1996) Resistance gene-dependent plant defense responses. Plant Cell **8:** 1773–1791

Hurkman WJ, Tanaka CK (1986) Solubilization of plant membrane proteins for analysis by two-dimensional gel electrophoresis. Plant Physiol **81:** 802–806

Iqbal MJ, Ahsan R, Afzal AJ, Jamai A, Meksem K, El Shemy H, Lightfoot DA (2009) Analysis of the activity of the soybean laccase encoded within the *Rfs2/rhg1* locus. Curr Issues Mol Biol **11:** 11–19

Ithal N, Recknor J, Nettleton D, Hearne L, Maier T, Baum TJ, Mitchum MG (2007a) Parallel genome-wide expression profiling of host and pathogen during soybean cyst nematode infection of soybean. Mol Plant Microbe Interact **20:** 293–305

Ithal N, Recknor J, Nettleton D, Maier T, Baum TJ, Mitchum MG (2007b) Developmental transcript profiling of cyst nematode feeding cells in soybean roots. Mol Plant Microbe Interact **20:** 510–525

Ito H, Iwabuchi M, Ogawa K (2003) The sugar-metabolic enzymes aldolase and triose-phosphate isomerase are targets of glutathionylation in *Arabidopsis thaliana*: detection using biotinylated glutathione. Plant Cell Physiol **44:** 655–660

Keen NT (1992) The molecular biology of disease resistance. Plant Mol Biol **19:** 109–122

Kemp BP, Beeching JR, Cooper RM (2005) cDNA-AFLP reveals genes differentially expressed during the hypersensitive response of cassava. Mol Plant Pathol **6:** 113–123

Kingston-Smith AH, Foyer CH (2000) Over-expression of Mn-superoxide dismutase in maize leaves leads to increased monodehydroascorbate reductase, dehydroascorbate reductase and glutathione reductase activities. J Exp Bot **51:** 1867–1877

Kirche HH, Bartels D, Wei YL, Schnable PS, Wood AJ (2004) The ALDH gene superfamily of *Arabidopsis*. Trends Plant Sci **9:** 371–377

Klink VP, Alkharouf N, MacDonald M, Matthews B (2005) Laser capture microdissection (LCM) and expression analyses of *Glycine max* (soybean) syncytium containing root regions formed by the plant pathogen *Heterodera glycines* (soybean cyst nematode). Plant Mol Biol **59:** 965–979

Klink VP, Overall CC, Alkharouf NW, Macdonald MH, Matthews BF (2007a) Laser capture microdissection (LCM) and comparative microarray expression analysis of syncytial cells isolated from incompatible and compatible soybean (*Glycine max*) roots infected by the soybean cyst nematode (*Heterodera glycines*). Planta **226:** 1389–1409

Klink VP, Overall CC, Alkharouf NW, Macdonald MH, Matthews BF (2007b) A time-course comparative microarray analysis of an incompatible and compatible response by *Glycine max* (soybean) to *Heterodera glycines* (soybean cyst nematode) infection. Planta **226:** 1423–1447

Kuc J (1995) Phytoalexins, stress metabolism, and disease resistance in plants. Annu Rev Phytopathol **33:** 275–297

Lee J, Bricker TM, Lefevre M, Pinson SRM, Oard JH (2006) Proteomic and genetic approaches to identifying defence-related proteins in rice challenged with the fungal pathogen *Rhizoctonia solani*. Mol Plant Pathol **7:** 405–416

Lei Z, Elmer AM, Watson BS, Dixon RA, Mendes PJ, Sumner LW (2005) A two-dimensional electrophoresis proteomic reference map and systematic identification of 1,367 proteins from a cell suspension culture of the model legume *Medicago truncatula*. Mol Cell Proteomics **4:** 1812–1825

Li CW, Bai YL, Jacobsen E, Visser R, Lindhout P, Bonnema G (2006) Tomato defense to the powdery mildew fungus: differences in expression of genes in susceptible, monogenic- and polygenic resistance responses are mainly in timing. Plant Mol Biol **62:** 127–140

Liu YL, Ahn JE, Datta S, Salzman RA, Moon J, Huyghues-Despointes B, Pittendrigh B, Murdock LL, Koiwa H, Zhu-Salzman K (2005) Arabidopsis vegetative storage protein is an anti-insect acid phosphatase. Plant Physiol **139:** 1545–1556

Livak KJ, Schmittgen TD (2001) Analysis of relative gene expression data using real-time quantitative PCR and the $2^{-\Delta\Delta CT}$ method. Methods **25:** 402–408

Marrs KA (1996) The functions and regulation of glutathione S-transferases in plants. Annu Rev Plant Physiol Plant Mol Biol **47:** 127–158

Martin GB, Bogdanove AJ, Sessa G (2003) Understanding the functions of plant disease resistance proteins. Annu Rev Plant Biol **54:** 23–61

Matvienko M, Wojtowicz A, Wrobel R, Jamison D, Goldwasser Y, Yoder JI (2001) Quinone oxidoreductase message levels are differentially regulated in parasitic and non-parasitic plants exposed to allelopathic quinones. Plant J **25:** 375–387

McManus MT, Burgess EPJ, Philip B, Watson LM, Laing WA, Voisey CR, White DWR (1999) Expression of the soybean (Kunitz) trypsin inhibitor in transgenic tobacco: effects on larval development of *Spodoptera litura*. Transgenic Res **8:** 383–395

Meksem K, Pantazopoulos P, Njiti VN, Hyten LD, Arelli PR, Lightfoot DA (2001) 'Forrest' resistance to the soybean cyst nematode is bigenic: saturation mapping of the *Rhg1* and *Rhg4* loci. Theor Appl Genet **103:** 710–717

Messina MJ, Liu KS (1997) Soybeans: Chemistry, Technology, and Utilization. Chapman & Hall/International Thompson Publishing, New York

Mitsui S, Wakasugi T, Hanano S, Sugiura M (1997) Localization of a cytokinin-binding protein CBP57/S-adenosyl-L-homocysteine hydrolase in a tobacco root. J Plant Physiol **150:** 752–754

Molloy MP, Herbert BR, Walsh BJ, Tyler MI, Traini M, Sanchez JC, Hochstrasser DF, Williams KL, Gooley AA (1998) Extraction of membrane proteins by differential solubilization for separation using two-dimensional gel electrophoresis. Electrophoresis **19:** 837–844

Mooney BP, Thelen JJ (2004) High-throughput peptide mass fingerprinting of soybean seed proteins: automated workflow and utility of UniGene expressed sequence tag databases for protein identification. Phytochemistry **65:** 1733–1744

Moy P, Qutob D, Chapman BP, Atkinson I, Gijzen M (2004) Patterns of gene expression upon infection of soybean plants by *Phytophthora sojae*. Mol Plant Microbe Interact **17:** 1051–1062

Mungur R (2008) Characterisation of Florigenic Signals between Plant Systems: A Tissue-Specific and Spatio-Temporal Analysis. Verlag Dr Mueller Press, Saarbrucken, Germany

Mysore KS, D'Ascenzo MD, He X, Martin GB (2003) Over-expression of the disease resistance gene *Pto* in tomato induces gene expression changes similar to immune responses in human and fruitfly. Plant Physiol **132:** 1901–1912

Naqvi SMS, Park KS, Yi SY, Lee HW, Bok SH, Choi D (1998) A glycine-rich RNA-binding protein gene is differentially expressed during acute hypersensitive response following tobacco mosaic virus infection in tobacco. Plant Mol Biol **37:** 571–576

Niblack TL, Tylka GL, Riggs RD (2004) Nematode pathogens of soybean. *In* HR Boerma, JE Specht, eds, Soybeans: Improvement, Production, and Uses, Ed 3. ASA-CSSA-SSSA, Madison, WI, pp 821–851

Nombela G, Williamson VM, Muñiz M (2003) The root-knot nematode resistance gene Mi-1.2 of tomato is responsible for resistance against the whitefly *Bemisia tabaci*. Mol Plant Microbe Interact **16:** 645–649

Park DS, Graham MY, Graham TL (2001) Identification of soybean elicitation competency factor, CF-1, as the soybean Kunitz trypsin inhibitor. Physiol Mol Plant Pathol **59:** 265–273

Puthoff DP, Nettleton D, Rodermel SR, Baum TJ (2003) Arabidopsis gene expression changes during cyst nematode parasitism showed by statistical analyses of microarray expression profiles. Plant J **33:** 911–921

Ralph S, Park JY, Bohlmann J, Mansfield SD (2006) Dirigent proteins in conifer defense: gene discovery, phylogeny, and differential wound- and insect-induced expression of a family of DIR and DIR-like genes in spruce (*Picea* spp.). Plant Mol Biol **60:** 21–40

Remm M, Storm CEV, Sonnhammer ELL (2001) Automatic clustering of orthologs and in-paralogs from pairwise species comparisons. J Mol Biol **314:** 1041–1052

Roggero P, Pennazio S (2008) The extracellular acidic and basic pathogenesis-related proteins of soybean induced by viral infection. J Phytopathol **127:** 274–280

Ruben E, Aziz J, Afzal J, Njiti VN, Triwitayakorn K, Iqbal MJ, Yaegashi S, Arelli P, Town C, Meksem K, et al (2006) Genomic analysis of the 'Peking' *rhg1* locus: candidate genes that underlie soybean resistance to the cyst nematode. Mol Genet Genomics **276:** 320–330

Sangster TA, Queitsch C (2005) The HSP90 chaperone complex, an emerging force in plant development and phenotypic plasticity. Curr Opin Plant Biol **8:** 86–92

Schad M, Mungur R, Fiehn O, Kehr J (2005) Metabolic profiling of laser micro-dissected vascular bundles of *Arabidopsis thaliana*. Plant Methods **1:** 2

Schmelz EA, Carroll MJ, LeClere S, Phipps SM, Meredith J, Chourey PS, Alborn HT, Teal PEA (2006) Fragments of ATP synthase mediate plant perception of insect attack. Proc Natl Acad Sci USA **103:** 8894–8899

Schmelz EA, LeClere S, Carroll MJ, Alborn HT, Teal PEA (2007) Cowpea chloroplastic ATP synthase is the source of multiple plant defense elicitors during insect herbivory. Plant Physiol **144:** 793–805

Seevers PM, Daly JM, Catedral FF (1971) The role of peroxidase isozymes in resistance to wheat stem rust disease. Plant Physiol **48:** 353–360

Sheffield J, Taylor N, Fauquet C, Chen SX (2006) The cassava (*Manihot esculenta* Crantz) root proteome: protein identification and differential expression. Proteomics **6:** 1588–1598

Shukla A, Bhaumik S, El-Shemy HA, Lightfoot DA (2009) The interactions of the largest subunit of RNA polymerase II with other cellular proteins: a bioinformatic approach. Curr Issues Mol Biol **11:** i65–i71

Sung DY, Guy CL (2003) Physiological and molecular assessment of altered expression of Hsc70-1 in Arabidopsis: evidence for pleiotropic consequences. Plant Physiol **132:** 979–987

Takahashi A, Casais C, Ichimura K, Shirasu K (2003) HSP90 interacts with RAR1 and SGT1 and is essential for RPS2-mediated disease resistance in Arabidopsis. Proc Natl Acad Sci USA **100:** 11777–11782

Testa B (1995) The Metabolism of Drugs and Other Xenobiotics. Academic Press, New York

Thimm O, Blasing O, Gibon Y, Nagel A, Meyer S, Kruger P, Selbig J, Muller LA, Rhee SY, Stitt M (2004) MAPMAN: a user-driven tool to display genomics data sets onto diagrams of metabolic pathways and other biological processes. Plant J **37:** 914–939

Tian AG, Wang J, Cui P, Han YJ, Xu H, Cong LJ, Huang XG, Wang XL, Jiao YZ, Wang BJ, et al (2004) Characterization of soybean genomic features by analysis of its expressed sequence tags. Theor Appl Genet **108:** 903–913

Triwitayakorn K, Njiti VN, Iqbal MJ, Yaegashi S, Town CD, Lightfoot DA (2005) Genomic analysis of a region encompassing *QRfs1* and *QRfs2*: genes that underlie soybean resistance to sudden death syndrome. Genome **48:** 125–138

Trudel J, Grenier J, Potvin C, Asselin A (1998) Several thaumatin-like proteins bind to β-1,3-glucans. Plant Physiol **118:** 1431–1438

Tyagi M, Kayastha AM, Sinha B (2000) The role of peroxidase and polyphenol oxidase isozymes in wheat resistance to *Alternaria triticina*. Biol Plant **43:** 559–562

Wan J, Torres M, Ganapathy A, Thelen J, DaGue BB, Mooney B, Xu D, Stacey G (2005) Proteomic analysis of soybean root hairs after infection by *Bradyrhizobium japonicum*. Mol Plant Microbe Interact **18:** 458–467

Wrather JA, Anderson TR, Arsyad DM, Gai J, Ploper DL, Portapuglia A, Ram HH, Yorinori JT (1996) Soybean disease loss estimates for the top ten producing countries during 1994. Plant Dis **79:** 107–111

Xu CP, Garrett WM, Sullivan J, Caperna TJ, Natarajan S (2006) Separation and identification of soybean leaf proteins by two-dimensional gel electrophoresis and mass spectrometry. Phytochemistry **67:** 2431–2440

Yu EZ, Burba AE, Gerstein M (2007) PARE: a tool for comparing protein abundance and mRNA expression data. BMC Bioinformatics **8:** 309

Yuan J, Njiti VN, Meksem K, Iqbal MJ, Triwitayakorn K, Kassem MA, Davis GT, Schmidt ME, Lightfoot DA (2002) Quantitative trait loci in two soybean recombinant inbred line populations segregating for yield and disease resistance. Crop Sci **42:** 271–277